โครงการ

การเรียนการสอนเพื่อเสริมประสบการณ์

ชื่อโครงการ การจำลองตัวแบบสมการเชิงอนุพันธ์สโตแคสติกสำหรับการตอบสนองต่อสิ่งกระตุ้นของเซลล์แกรนูลในสมองส่วนซีรีเบลลัม
Simulations of Stochastic Differential Equation Model for Cerebellar Granule Cell Excitability

ชื่อนิสิต นาย ศรทรรศณ์ กวินนิธิพันธ์ 5833523523

ภาควิชา คณิตศาสตร์และวิทยาการคอมพิวเตอร์
สาขาวิชา คณิตศาสตร์

ปีการศึกษา 2561

คณะวิทยาศาสตร์ จุฬาลงกรณ์มหาวิทยาลัย

การจำลองตัวแบบสมการเชิงอนุพันธ์สโตแคสติกสำหรับการตอบสนองต่อสิ่งกระตุ้นของเซลล์แกรนูลในสมองส่วนซีรีเบลลัม

นายศรทรรศณ์ กวินนิธิพันธ์

โครงงานนี้เป็นส่วนหนึ่งของการศึกษาตามหลักสูตรวิทยาศาสตรบัณฑิต
สาขาวิชาคณิตศาสตร์ ภาควิชาคณิตศาสตร์และวิทยาการคอมพิวเตอร์
คณะวิทยาศาสตร์ จุฬาลงกรณ์มหาวิทยาลัย
ปีการศึกษา 2561

Simulations of Stochastic Differential Equation Model for Cerebellar Granule Cell Excitability

Mr. Sorntuss Kawinnitipan

A Project Submitted in Partial Fulfillment of the Requirements
for the Degree of Bachelor of Science Program in Mathematics
Department of Mathematics and Computer Science
Faculty of Science
Chulalongkorn University
Academic Year 2018

หัวข้อโครงงาน	การจำลองตัวแบบสมการเชิงอนุพันธ์สโตแคสติกสำหรับการตอบสนองต่อสิ่งกระตุ้นของเซลล์แกรนูลในสมองส่วนซีรีเบลลัม
โดย	นายศรทรรศณ์ กวินนิธิพันธ์ เลขประจำตัว 5833523523
สาขาวิชา	คณิตศาสตร์
อาจารย์ที่ปรึกษาโครงงาน	อาจารย์ ดร. เรวัต ถนัดกิจหิรัญ

ภาควิชาคณิตศาสตร์และวิทยาการคอมพิวเตอร์ คณะวิทยาศาสตร์ จุฬาลงกรณ์มหาวิทยาลัย อนุมัติให้นับโครงงานฉบับนี้เป็นส่วนหนึ่ง ของการศึกษาตามหลักสูตรปริญญาบัณฑิต ในรายวิชา 2301499 โครงงานวิทยาศาสตร์ (Senior Project)

..... หัวหน้าภาควิชาคณิตศาสตร์
และวิทยาการคอมพิวเตอร์

(ศาสตราจารย์ ดร.กฤษณะ เนียมมณี)

คณะกรรมการสอบโครงงาน

..... อาจารย์ที่ปรึกษาโครงงาน

(อาจารย์ ดร. เรวัต ถนัดกิจหิรัญ)

..... กรรมการ

(ผู้ช่วยศาสตราจารย์ ดร.คำรณ เมฆฉาย)

..... กรรมการ

(ผู้ช่วยศาสตราจารย์ ดร. เพชรอาภา บุญเสริม)

ศรทรรศณ์ กวินนิธิพันธ์: การจำลองตัวแบบสมการเชิงอนุพันธ์สโตแคสติกสำหรับการตอบสนองต่อสิ่งกระตุ้นของเซลล์แกรนูลในสมองส่วนซีรีเบลลัม (SIMULATIONS OF STOCHASTIC DIFFERENTIAL EQUATION MODEL FOR CEREBELLAR GRANULE CELL EXCITABILITY) อ.ที่ปรึกษาโครงงาน: อาจารย์ ดร. เรวัต ฉนัดกิจหิรัญ, 31 หน้า

การจำลองตัวแบบสมการเชิงอนุพันธ์สโตแคสติกสำหรับการตอบสนองต่อสิ่งกระตุ้นของเซลล์แกรนูลในสมองส่วนซีรีเบลลัมคือการศึกษาพฤติกรรมการเปลี่ยนแปลงของเซลล์สมองซึ่งสามารถเขียนได้ในเชิงอนุพันธ์สโตแคสติกตามธรรมชาติ โดยโครงงานนี้ได้ศึกษาโมเดลต้นแบบของการเปลี่ยนแปลงพฤติกรรมโดยใช้ตัวไอออนจากไอออนแชนแนลในเซลล์สมองและตัวความเข้มข้นของแคลเซียม ในโครงงานนี้ได้ทำการปรับโมเดลโดยการเพิ่มสมการกระบวนการบางอย่างลงไปในพจน์ของดิฟฟิวชั่นของตัวโมเดลและทำการศึกษาผลในสามด้านของทั้ง 2 โมเดล ได้แก่ 1.) ผลของสัญญาณไฟฟ้าในสมองต่ออัตราการเกิดสไปค์ 2.) ความหลากหลายของสไปค์ในช่วงเวลา 3.) ระยะห่างของแต่ละช่วงของการเกิดจุดยอด

ภาควิชา คณิตศาสตร์และวิทยาการคอมพิวเตอร์ ลายมือชื่อนิสิต ศรทรรศณ์ กวินนิธิพันธ์

สาขาวิชา . คณิตศาสตร์ . ลายมือชื่อ อ.ที่ปรึกษาโครงงาน เรวัต ฉนัดกิจหิรัญ

ปีการศึกษา . . . . 2561 . . . .

5833523523 : MAJOR MATHEMATICS.
KEYWORDS: STOCHASTIC DIFFERENTIAL EQUATION, CEREBELLAR GRANULE CELL, ION CHANNEL, EULER MARUYAMA, NEURONS
SORNTHUSS KAWINNITIPAN: SIMULATIONS OF STOCHASTIC DIFFERENTIAL EQUATION MODEL FOR CEREBELLAR GRANULE CELL EXCITABILITY.
ADVISOR: RAYWAT TANADKITHIRUN, PH.D., 31 PP.

Simulations of stochastic differential equation model for cerebellar granule cell excitability study about neurons in the brain intrinsic dynamic behavior which is known to be stochastic in nature. In this project, we study a prototype model of dynamic behavior by using ions in ion channels and calcium concentration. We also try to adjust the original model by adding some processes into the diffusion parts of the model. We analyze the results for both model in three aspects which are 1.) the effect of electrical signal to the spike timing, 2.) the variability in spike timing, and 3.) interspike intervals.

Department . Mathematics and Computer Science . Student's Signature .....
Field of Study . . Mathematics . . Advisor's Signature .....
Academic Year . . . . . 2018 . . . . .

Acknowledgements

I would like to express my sincere gratitude to my project advisor, Raywat Tanadkithirun, Ph.D., for providing invaluable guidance, comments, and suggestions throughout the course of this project. I could not have imagined having a better advisor and mentor for my project. Besides my advisor, I would like to express my special thanks to my project committees, Assistant Professor Khamron Mekchay, Ph.D. and Assistant Professor Petarpa Boonserm, Ph.D., for their encouragement, insightful comments, and good questions. Moreover, I feel very thankful to all of my teachers who have taught me abundant knowledge. Last but not least, I would like to thank my family for supporting me spiritually throughout my life.

Contents

List of Figures

Chapter 1

Introduction

Neurons are electrically excitable cells that receive, process, and transmit information through electrical and chemical signals. Neurons in the brain express intrinsic dynamic behavior which is known to be stochastic in nature. Cerebellar granule cells are the most abundant neurons in the human brain and are among the smallest neurons in the brain.

In the cell membrane, many ions have a concentration gradient across the membrane. Some ions have high concentration inside the membrane but low concentration outside the membrane, and vice versa. These concentration gradients provide the potential energy to drive the formation of the membrane potential. This voltage is established when the membrane has permeability to one or more ions.

Ion channels are pore-forming membrane proteins that allow ions to pass through the channel pore. Due to random opening and closing (gating) of an ion channel at an experimentally fixed membrane potential, Saarinen et al. [2] propose a system of stochastic differential equations (SDEs) to model the intrinsic dynamic behavior of cerebellar granule cells. This model includes six different types of voltage-dependent conductances: the fast inactivating sodium channel (Na_F), the delayed rectifier potassium channel (K_{D_r}), the transient A-type potassium channel (K_A), the inward rectifier potassium channel (K_{i_r}), the high-voltage-activated calcium channel (Ca_{HVA}), and the large-conductance calcium and voltage-activated potassium channel (BK_{ca}) as well as simple calcium dynamics to describe the change in membrane potential.

In [1], Marja-Leena Linne and her team used Hodgkin-Huxley for model for ion channel/current behavior and a simple model for calcium dynamics and describe the granule neuron excitability. The starting parameter values of the model equation were selected based on data from in vitro experiments on cerebellar granule neurons. The basic excitability properties of the granule neuron were used as the main constraints of the model. In the experiment, the neuron was assumed as one-compartmental sphere which containing six different voltage-dependent ion channel/ current types (Na_F, K_{D_r},K_A, K_{i_r}, Ca_{HVA}, BK_{ca}).

The change in membrane potential is described from [2] by the system of SDEs

$$
\left.\begin{aligned}
dV_m(t) &= \frac{1}{C_m}\Big(I_{app} - G_1 x_1^{p_1}(t)x_2^{q_1}(t)(V_m(t)-E_1) \\
&\qquad - G_2 x_3^{p_2}(t)(V_m(t)-E_2) - G_3 x_4^{p_3}(t)x_5^{q_3}(t)(V_m(t)-E_3) \\
&\qquad - G_4 x_6^{p_4}(t)(V_m(t)-E_4) - G_5 x_7^{p_5}(t)x_8^{q_5}(t)(V_m(t)-E_5) \\
&\qquad - G_6 x_9^{p_6}(t)(V_m(t)-E_6) - \frac{1}{R_m}(V_m(t)-E_m)\Big)dt, \\
dx_1(t) &= \big(\alpha_1(V_m(t))(1-x_1(t)) - \beta_1(V_m(t))x_1(t)\big)dt + \sigma_1 dW_1(t), \\
dx_2(t) &= \big(\alpha_2(V_m(t))(1-x_2(t)) - \beta_2(V_m(t))x_2(t)\big)dt + \sigma_2 dW_2(t), \\
dx_3(t) &= \big(\alpha_3(V_m(t))(1-x_3(t)) - \beta_3(V_m(t))x_3(t)\big)dt + \sigma_3 dW_3(t), \\
dx_4(t) &= \big(\alpha_4(V_m(t))(1-x_4(t)) - \beta_4(V_m(t))x_4(t)\big)dt + \sigma_4 dW_4(t), \\
dx_5(t) &= \big(\alpha_5(V_m(t))(1-x_5(t)) - \beta_5(V_m(t))x_5(t)\big)dt + \sigma_5 dW_5(t), \\
dx_6(t) &= \big(\alpha_6(V_m(t))(1-x_6(t)) - \beta_6(V_m(t))x_6(t)\big)dt + \sigma_6 dW_6(t), \\
dx_7(t) &= \big(\alpha_7(V_m(t))(1-x_7(t)) - \beta_7(V_m(t))x_7(t)\big)dt + \sigma_7 dW_7(t), \\
dx_8(t) &= \big(\alpha_8(V_m(t))(1-x_8(t)) - \beta_8(V_m(t))x_8(t)\big)dt + \sigma_8 dW_8(t), \\
dx_9(t) &= \big(\alpha_9(V_m(t),x_{10}(t))(1-x_9(t)) - \beta_9(V_m(t),x_{10}(t))x_9(t)\big)dt + \sigma_9 dW_9(t), \\
dx_{10}(t) &= \Big(\frac{B\,G_5 x_7^{p_5}(t)x_8^{q_5}(t)(V_m(t)-E_5)}{\pi\, dcell^2\, dshell} - \frac{x_{10}(t)-[Ca^{2+}]_{rest}}{\tau_{Ca}}\Big)dt,
\end{aligned}\right\} \quad (1)
$$

where $V_m(t)$ is the process of membrane potential,

$x_1(t)$ is the activation process for Na_F ion channel,

$x_2(t)$ is the inactivation process for Na_F ion channel,

$x_3(t)$ is the activation process for K_{Dr} ion channel,

$x_4(t)$ is the activation process for K_A ion channel,

$x_5(t)$ is the inactivation process for K_A ion channel,

$x_6(t)$ is the activation process for K_ir ion channel,

$x_7(t)$ is the activation process for Ca_{HVA} ion channel,

$x_8(t)$ is the inactivation process for Ca_{HVA} ion channel,

$x_9(t)$ is the activation process for BK_{ca} ion channel,

$x_{10}(t)$ is the process for intercellular calcium (Ca^{2+} ions) concentration,

α_i and β_i are the coefficient functions for $i = 1, 2, \ldots, 9$ given by

$$\alpha_1(V_m(t)) = 3 \cdot 10^3 e^{\left((V_m(t)-0.01)+39\cdot 10^{-3}\right)\cdot 0.081\cdot 10^3},$$

$$\beta_1(V_m(t)) = 3 \cdot 10^3 e^{\left((V_m(t)-0.01)+39\cdot 10^{-3}\right)\cdot -0.066\cdot 10^3},$$

$$\alpha_2(V_m(t)) = 0.24 \cdot 10^3 e^{\left((V_m(t)-0.01))+50\cdot 10^{-3}\right)\cdot -0.089\cdot 10^3},$$

$$\beta_2(V_m(t)) = 0.24 \cdot 10^3 e^{\left((V_m(t)-0.01)+50\cdot 10^{-3}\right)\cdot 0.089\cdot 10^3},$$

$$\alpha_3(V_m(t)) = 0.34 \cdot 10^3 e^{\left((V_m(t)-0.01)+38\cdot 10^{-3}\right)\cdot 0.073\cdot 10^3},$$

$$\beta_3(V_m(t)) = 0.34 \cdot 10^3 e^{\left((V_m(t)-0.01)+38\cdot 10^{-3}\right)\cdot -0.018\cdot 10^3},$$

$$\alpha_4(V_m(t)) = 2.2 \cdot 10^3 e^{\left((V_m(t)-0.01)+46.7\cdot 10^{-3}\right)\cdot 0.04\cdot 10^3},$$

$$\beta_4(V_m(t)) = 2.2 \cdot 10^3 e^{\left((V_m(t)-0.01)+46.7\cdot 10^{-3}\right)\cdot -0.01\cdot 10^3},$$

$$\alpha_5(V_m(t)) = 0.016 \cdot 10^3 e^{\left((V_m(t)-0.01)+78.8\cdot 10^{-3}\right)\cdot -0.075\cdot 10^3},$$

$$\beta_5(V_m(t)) = 0.016 \cdot 10^3 e^{\left((V_m(t)-0.01)+78.8\cdot 10^{-3}\right)\cdot 0.055\cdot 10^3},$$

$$\alpha_6(V_m(t)) = 0.133 \cdot 10^3 e^{\left((V_m(t)-0.01)+83.94\cdot 10^{-3}\right)\cdot -0.0411\cdot 10^3},$$

$$\beta_6(V_m(t)) = 0.17 \cdot 10^3 e^{\left((V_m(t)-0.01)+83.94\cdot 10^{-3}\right)\cdot 0.028\cdot 10^3},$$

$$\alpha_7(V_m(t)) = 0.049 \cdot 10^3 e^{\left((V_m(t)-0.01)+29.06\cdot 10^{-3}\right)\cdot 0.063\cdot 10^3},$$

$$\beta_7(V_m(t)) = 0.082 \cdot 10^3 e^{\left((V_m(t)-0.01)+18.66\cdot 10^{-3}\right)\cdot -0.039\cdot 10^3},$$

$$\alpha_8(V_m(t)) = 0.0013 \cdot 10^3 e^{\left((V_m(t)-0.01)+48\cdot 10^{-3}\right)\cdot -0.055\cdot 10^3},$$

$$\beta_8(V_m(t)) = 0.0013 \cdot 10^3 e^{\left((V_m(t)-0.01)+48\cdot 10^{-3}\right)\cdot 0.012102142\cdot 10^3},$$

$$\alpha_9(V_m(t), x_{10}(t)) = \frac{2.5 \cdot 10^3}{1 + 1.5 \cdot 10^{-3} \cdot e^{-0.085\cdot 10^3 (V_m(t)-0.01)}/x_{10}(t)},$$

$$\beta_9(V_m(t), x_{10}(t)) = \frac{1.5 \cdot 10^3}{1 + x_{10}(t)/(150 \cdot 10^{-6} \cdot e^{-0.077\cdot 10^3 (V_m(t)-0.01)})},$$

C_m, G_1, G_2, G_3, G_4, G_5, G_6, p_1, q_1, p_2, p_3, q_3, p_4, p_5, q_5, p_6, E_1, E_2 ,E_3, E_4, E_5, E_6, E_m, R_m, B, τ_{Ca} , $dcell$, $dshell$ and $[Ca^{2+}]_{rest}$ are constant parameters in the model given in figure 1.1, I_{app} is an applied current, and σ_i for for $i = 1, 2, \ldots, 9$ are the parameter

that bring the intensity of random fluctuations.

All of these processes occur at membrane called an ion channel. Each ion has its own channel but some channels can allow more than two ions to pass. From now on, we will call the processes x_i for $i = 1, 2, \ldots, 9$ the gating variables.

In this work, we choose electrical signal to study. In our brain, neurons express intrinsic dynamic behavior which is known to be stochastic in nature. A neuron cell has membrane and many ions. When neurons send some information by using electrical signal, they use ions to be a conductor. Electrical signal is an applied current (I_{app}) which is used to transmit information in neurons, and we use three values of I_{app} which are 11, 12 and 29 cA. The applied current with ions moves into the membrane or moves out from the membrane to other cells so these cause the change in membrane potential, $V_m(t)$. We also add stochasticity into gating variables ($x_i(1 - x_i)$) to obtain another model and we will simulate the process $V_m(t)$ by using the Euler-Maruyama method and use the result to analyze the variability in spike timing and use the result from the simulation of interspike intervals to see variability in the firing caused by the parameter σ_i.

Constant	Value	Description
R_m	0.57 Ωm^2	membrane resistance
C_m	0.03 F/m^2	membrane capacity
E_m	-0.025 V	equilibrium membrane potential
E_1	+0.07 V	equilibrium potential for Na^+
$E_2 = E_3 = E_4$	-0.075 V	equilibrium potential for K^+
E_5	+0.14 V	equilibrium potential for Ca^{2+}
E_6	-0.085 V	equilibrium potential for BK_{Ca}
B	$5.2 \cdot 10^{-6}$mol/C	constant for Ca^{2+} transfer into the cell
$[Ca^{2+}]_{rest}$	$100 \cdot 10^{-6}$mol/m^3	$[Ca^{2+}]$ at rest
τ_{ca}	$1 \cdot 10^{-3}$s	time constant for the decay of intracellular free calcium
dcell	$6 \cdot 10^{-6}$m	diameter of the granule cell
dshell	$1 \cdot 10^{-7}$m	diameter of the shell defining the volume In which calcium ions are processed
G_1	400 S/m^2	maximal conductance for Na_F
G_2	120 S/m^2	maximal conductance for K_{Dr}
G_3	10 S/m^2	maximal conductance for K_A
G_4	28 S/m^2	maximal conductance for K_{ir}
G_5	4.6 S/m^2	maximal conductance for Ca_{HVA}
G_6	30 S/m^2	maximal conductance for BK_{Ca}
p_1	3	exponential for Na_F activation
q_1	1	exponential for Na_F inactivation
p_2	4	exponential for K_{Dr} activation
p_3	3	exponential for K_A activation
q_3	1	exponential for K_A inactivation
p_4	1	exponential forK_{ir}activation
p_5	2	exponential for Ca_{HVA} activation
q_5	1	exponential for Ca_{HVA} inactivation
p_6	1	exponential for BK_{Ca} activation

Figure 1.1: Constant parameters in the original model.

Chapter 2

Background Knowledge

In this chapter, we describe the background knowledge and the concept for our project which are stochastic differential equations and the numerical method that we will use in this work.

2.1 Stochastic differential equation

Definition 2.1.1. *The Wiener process* $\{W_t\}_{t\in[0,T]}$ *is a stochastic process characterised by the following properties.*

1. $W_0 = 0$ *with probability* 1.
2. *For* $0 \leq s \leq t \leq T$*, the random variable given by the increment* W_t - W_s *is normally distributed with mean zero and variance* $t - s$*, or equivalently,* W_t - $W_s \sim \sqrt{t-s}\, N(0,1)$.
3. *For* $0 \leq s < t \leq u < v \leq T$*, the increments* W_t - W_s *and* W_v - W_u *are independent.*
4. *It has continuous sample paths with probability* 1.

Definition 2.1.2. *A stochastic differential equation (SDE) has the form*

$$\begin{aligned} dX_t &= a(X_t,t)dt + b(X_t,t)dW_t, \qquad 0 \leq t \leq T \\ X_0 &= x, \end{aligned} \tag{2.1}$$

where W_t denotes a Wiener process, a and b are scalar functions of X_t, and $x \in \mathbb{R}$. The equation (2.1) is understood to be the differential form of the integral equation

$$X_t - X_0 = \int_0^t f(X_s, s)ds + \int_0^t g(X_s, s)dW_s \tag{2.2}$$

where the first term on the right-hand side of the above equation is interpreted as the ordinary Riemann integral, and the second term is the Ito integral.

2.2 The Euler-Maruyama method

The simplest numerical approximation for solving an SDE is the Euler-Maruyama method. We need to discretize the time domain $[0, T]$ into N equidistance subintervals. Let $t_n = n\triangle$ for all $n = 0, 1, \ldots, N$ where $\triangle = \frac{T}{N}$. We denote x_n to be the numerical solution at time step t_n using the Euler-Maruyama scheme

$$x_{n+1} = x_n + f(x_n)\triangle + g(x_n)\triangle W_n$$

where $\triangle W_n$ is normally distributed with mean 0 and variance $\triangle$ and $x_0 = X_0$. We simulate for each x_n from the time domain $[0, T]$, so we get x_0 at time 0 until x_N at time T. Then, we have one sample path. If we do the simulation agian, we will not get the same sample path because we generate other random numbers.

Chapter 3

Methodology

In this chapter, we will use a numerical method to find the numerical solution of the change in membrane potential $V_m(t)$.

3.1 Our model

We simulate the original model (1) and our model. From a suggestion in [2], Marja-Leena Linne and her team gave an advice which is adding some function of gating variables to reduce noises that will be outside the interval [0,1]. Each value in the range [0,1] tells the status of the ion channel whether it is open or closed. When the channel is fully open, this value is set to 1, and when the channel is completely closed, this value is set to 0. However, Marja-Leena Linne and her team did not tell what is the appropriate functions of gating variables so we decide to add the term $x_i(t)(1-x_i(t))$ at the random term for each SDE in the original model to be our proposed model. We expect that the term $x_i(t)(1-x_i(t))$ will reduce noises near 0 and 1 and make our model appropriate to simulate the change in membrane potential. Note that, in this work, we actually restrict all of the process $x_i(t)$ to live in the interval $[0,1]$.

Our model has the form

$$
\left.\begin{aligned}
dV_m(t) &= \frac{1}{C_m}\Big(I_{app} - G_1 x_1^{p_1}(t)x_2^{q_1}(t)(V_m(t)-E_1) \\
&\qquad - G_2 x_3^{p_2}(t)(V_m(t)-E_2) - G_3 x_4^{p_3}(t)x_5^{q_3}(t)(V_m(t)-E_3) \\
&\qquad - G_4 x_6^{p_4}(t)(V_m(t)-E_4) - G_5 x_7^{p_5}(t)x_8^{q_5}(t)(V_m(t)-E_5) \\
&\qquad - G_6 x_9^{p_6}(t)(V_m(t)-E_6) - \frac{1}{R_m}(V_m(t)-E_m)\Big)dt, \\
dx_1(t) &= \big(\alpha_1(V_m(t))(1-x_1(t)) - \beta_1(V_m(t))x_1(t)\big)dt + \sigma_1 x_1(t)(1-x_1(t))dW_1(t), \\
dx_2(t) &= \big(\alpha_2(V_m(t))(1-x_2(t)) - \beta_2(V_m(t))x_2(t)\big)dt + \sigma_2 x_2(t)(1-x_2(t))dW_2(t), \\
dx_3(t) &= \big(\alpha_3(V_m(t))(1-x_3(t)) - \beta_3(V_m(t))x_3(t)\big)dt + \sigma_3 x_3(t)(1-x_3(t))dW_3(t), \\
dx_4(t) &= \big(\alpha_4(V_m(t))(1-x_4(t)) - \beta_4(V_m(t)x_4(t)\big)dt + \sigma_4 x_4(t)(1-x_4(t))dW_4(t), \\
dx_5(t) &= \big(\alpha_5(V_m(t))(1-x_5(t)) - \beta_5(V_m(t)x_5(t)\big)dt + \sigma_5 x_5(t)(1-x_5(t))dW_5(t), \\
dx_6(t) &= \big(\alpha_6(V_m(t))(1-x_6(t)) - \beta_6(V_m(t))x_6(t)\big)dt + \sigma_6 x_6(t)(1-x_6(t))dW_6(t), \\
dx_7(t) &= \big(\alpha_7(V_m(t))(1-x_7(t)) - \beta_7(V_m(t))x_7(t)\big)dt + \sigma_7 x_7(t)(1-x_7(t))dW_7(t), \\
dx_8(t) &= \big(\alpha_8(V_m(t))(1-x_8(t)) - \beta_8(V_m(t))x_8(t)\big)dt + \sigma_8 x_8(t)(1-x_8(t))dW_8(t), \\
dx_9(t) &= \big(\alpha_9(V_m(t),x_{10}(t))(1-x_9(t)) - \beta_9(V_m(t),x_{10}(t))x_9(t)\big)dt \\
&\qquad + \sigma_9 x_9(t)(1-x_9(t))dW_9(t), \\
dx_{10}(t) &= \Big(\frac{B\,G_5 x_7^{p_5}(t)x_8^{q_5}(t)(V_m(t)-E_5)}{\pi\, dcell^2\, dshell} - \frac{x_{10}(t)-[Ca^{2+}]_{rest}}{\tau_{Ca}}\Big)dt,
\end{aligned}\right\} \quad (2)
$$

where all processes, functions and all parameters in this model are as same as in equation (1).

3.2 Numerical method

In this project, we use MATLAB to find numerical solution by using Euler-Maruyama to simulate the process $V_m(t)$. We discretize the time domain $[0, T]$ into N equidistance subintervals. Let $t_n = n\triangle$ for all $n = 0, 1, \ldots, N$ where $\triangle = \frac{T}{N}$.

3.2.1 Euler-Maruyama scheme for the original model

The Euler-Maruyama scheme for the original model has the form

$$\begin{aligned}
V_n &= V_{n-1} + \frac{1}{C_m}\Big(I_{app} - G_1 x1_{n-1}^{p_1} x2_{n-1}^{q_1}(V_{n-1} - E_1) \\
&\quad - G_2 x3_{n-1}^{p_2}(V_{n-1} - E_2) - G_3 x4_{n-1}^{p_3} x5_{n-1}^{q_3}(V_{n-1} - E_3) \\
&\quad - G_4 x6_{n-1}^{p_4}(V_{n-1} - E_4) - G_5 x7_{n-1}^{p_5} x8_{n-1}^{q_5}(V_{n-1} - E_5) \\
&\quad - G_6 x9_{n-1}^{p_6}(V_{n-1} - E_6) - \frac{1}{R_m}(V_{n-1} - E_m)\Big)\triangle, \\
x1_n &= x1_{n-1} + \big[\alpha_1(V_{n-1})(1 - x1_{n-1}) - \beta_1(V_{n-1})x1_{n-1}\big]\triangle + \sigma\triangle W_1, \\
x2_n &= x2_{n-1} + \big[\alpha_2(V_{n-1})(1 - x2_{n-1}) - \beta_2(V_{n-1})x2_{n-1}\big]\triangle + \sigma\triangle W_2, \\
x3_n &= x3_{n-1} + \big[\alpha_3(V_{n-1})(1 - x3_{n-1}) - \beta_3(V_{n-1})x3_{n-1}\big]\triangle + \sigma\triangle W_3, \\
x4_n &= x4_{n-1} + \big[\alpha_4(V_{n-1})(1 - x4_{n-1}) - \beta_4(V_{n-1})x4_{n-1}\big]\triangle + \sigma\triangle W_4, \\
x5_n &= x5_{n-1} + \big[\alpha_5(V_{n-1})(1 - x5_{n-1}) - \beta_5(V_{n-1})x5_{n-1}\big]\triangle + \sigma\triangle W_5, \\
x6_n &= x6_{n-1} + \big[\alpha_6(V_{n-1})(1 - x6_{n-1}) - \beta_6(V_{n-1})x6_{n-1}\big]\triangle + \sigma\triangle W_6, \\
x7_n &= x7_{n-1} + \big[\alpha_7(V_{n-1})(1 - x7_{n-1}) - \beta_7(V_{n-1})x7_{n-1}\big]\triangle + \sigma\triangle W_7, \\
x8_n &= x8_{n-1} + \big[\alpha_8(V_{n-1})(1 - x8_{n-1}) - \beta_8(V_{n-1})x8_{n-1}\big]\triangle + \sigma\triangle W_8, \\
x9_n &= x9_{n-1} + \big[\alpha_9(V_{n-1}, x10_{n-1})(1 - x9_{n-1}) - \beta_9(V_{n-1}, x10_{n-1})x9_{n-1}\big]\triangle + \sigma\triangle W_9, \\
x10_n &= x10_{n-1} + \Big[\frac{B\,G_5 x7_{n-1}^{p_5} x8_{n-1}^{q_5}(V_{n-1} - E_5)}{\pi\, dcell^2\, dshell} - \frac{x10_{n-1} - [Ca^{2+}]_{rest}}{\tau_{Ca}}\Big]\triangle,
\end{aligned}$$

where $\triangle W_i \sim \mathcal{N}(0, \triangle)$ for all $i = 1, 2, .., 9$,

V_n is a numerical solution of $V_m(t_n)$,

$x1_n$ is a numerical solution of $x_1(t_n)$,

$x2_n$ is a numerical solution of $x_2(t_n)$,

$x3_n$ is a numerical solution of $x_3(t_n)$,

$x4_n$ is a numerical solution of $x_4(t_n)$,

$x5_n$ is a numerical solution of $x_5(t_n)$,

$x6_n$ is a numerical solution of $x_6(t_n)$,

$x7_n$ is a numerical solution of $x_7(t_n)$,

$x8_n$ is a numerical solution of $x_8(t_n)$,

$x9_n$ is a numerical solution of $x_9(t_n)$,

$x10_n$ is a numerical solution of $x_{10}(t_n)$,

for all $n = 1, 2, \ldots, N$.

3.2.2 Euler-Maruyama scheme for our new model

All values of parameters in our model are the same parameters in the original model. For our model, we will add a tilde accent on V_n, V_{n-1}, xi_n and xi_{n-1} for $i = 1, 2, \ldots, 10$ to denote the numerical solutions for our model. The Euler-Maruyama scheme for our model has the form

$$\begin{aligned}
\tilde{V_n} = \tilde{V}_{n-1} + \frac{1}{C_m}\Big[& I_{app} - G_1\tilde{x}1_{n-1}^{p_1}\tilde{x}2_{n-1}^{q_1}(\tilde{V}_{n-1} - E_1) \\
& - G_2\tilde{x}3_{n-1}^{p_2}(\tilde{V}_{n-1} - E_2) - G_3\tilde{x}4_{n-1}^{p_3}\tilde{x}5_{n-1}^{q_3}(\tilde{V}_{n-1} - E_3) \\
& - G_4\tilde{x}6_{n-1}^{p_4}(\tilde{V}_{n-1} - E_4) - G_5\tilde{x}7_{n-1}^{p_5}\tilde{x}8_{n-1}^{q_5}(\tilde{V}_{n-1} - E_5) \\
& - G_6\tilde{x}9_{n-1}^{p_6}(\tilde{V}_{n-1} - E_6) - \frac{1}{R_m}(\tilde{V}_{n-1} - E_m)\Big]\triangle, \\
\tilde{x}1_n = \tilde{x}1_{n-1} + & \big[\alpha_1(\tilde{V}_{n-1})(1 - \tilde{x}1_{n-1}) - \beta_1(\tilde{V}_{n-1})\tilde{x}1_{n-1}\big]\triangle \\
& + \sigma_1(\tilde{x}1_{n-1})(1 - \tilde{x}1_{n-1})\triangle W_1, \\
\tilde{x}2_n = \tilde{x}2_{n-1} + & \big[\alpha_2(\tilde{V}_{n-1})(1 - \tilde{x}2_{n-1}) - \beta_2(\tilde{V}_{n-1})\tilde{x}2_{n-1}\big]\triangle \\
& + \sigma_2(\tilde{x}2_{n-1})(1 - \tilde{x}2_{n-1})\triangle W_2, \\
\tilde{x}3_n = \tilde{x}3_{n-1} + & \big[\alpha_3(\tilde{V}_{n-1})(1 - \tilde{x}3_{n-1}) - \beta_3\tilde{V}_{n-1})\tilde{x}3_{n-1}\big]\triangle \\
& + \sigma_3(\tilde{x}3_{n-1})(1 - \tilde{x}3_{n-1})\triangle W_3, \\
\tilde{x}4_n = \tilde{x}4_{n-1} + & \big[\alpha_4(\tilde{V}_{n-1})(1 - \tilde{x}4_{n-1}) - \beta_4(\tilde{V}_{n-1})\tilde{x}4_{n-1}\big]\triangle \\
& + \sigma_4(\tilde{x}4_{n-1})(1 - \tilde{x}4_{n-1})\triangle W_4, \\
\tilde{x}5_n = \tilde{x}5_{n-1} + & \big[\alpha_5(\tilde{V}_{n-1})(1 - \tilde{x}5_{n-1}) - \beta_5(\tilde{V}_{n-1})\tilde{x}5_{n-1}\big]\triangle \\
& + \sigma_5(\tilde{x}5_{n-1})(1 - \tilde{x}5_{n-1})\triangle W_5, \\
\tilde{x}6_n = \tilde{x}6_{n-1} + & \big[\alpha_6(\tilde{V}_{n-1})(1 - \tilde{x}6_{n-1}) - \beta_6(\tilde{V}_{n-1})\tilde{x}6_{n-1}\big]\triangle \\
& + \sigma_6(\tilde{x}6_{n-1})(1 - \tilde{x}6_{n-1})\triangle W_6, \\
\tilde{x}7_n = \tilde{x}7_{n-1} + & \big[\alpha_7(\tilde{V}_{n-1})(1 - \tilde{x}7_{n-1}) - \beta_7(\tilde{V}_{n-1})\tilde{x}7_{n-1}\big]\triangle \\
& + \sigma_7(\tilde{x}7_{n-1})(1 - \tilde{x}7_{n-1})\triangle W_7, \\
\tilde{x}8_n = \tilde{x}8_{n-1} + & \big[\alpha_8(\tilde{V}_{n-1})(1 - \tilde{x}8_{n-1}) - \beta_8(\tilde{V}_{n-1})\tilde{x}8_{n-1}\big]\triangle \\
& + \sigma_8(\tilde{x}8_{n-1})(1 - \tilde{x}8_{n-1})\triangle W_8,
\end{aligned}$$

$$\tilde{x}9_n = \tilde{x}9_{n-1} + \big[\alpha_9(\tilde{V}_{n-1}, \tilde{x}10_{n-1})(1 - \tilde{x}9_{n-1}) - \beta_9(\tilde{V}_{n-1}, \tilde{x}10_{n-1})\tilde{x}9_{n-1}\big]\triangle$$
$$+ \sigma_9(\tilde{x}9_{n-1})(1 - \tilde{x}9_{n-1})\triangle W_9,$$
$$\tilde{x}10_n = \tilde{x}10_{n-1} + \Big[\frac{BG_5\tilde{x}7_{n-1}^{p_5}\tilde{x}8_{n-1}^{q_5}(\tilde{V}_{n-1} - E_5)}{\pi dcell^2 dshell} - \frac{\tilde{x}10_{n-1} - [Ca^{2+}]_{rest}}{\tau_{Ca}}\Big]\triangle,$$

where $\triangle W_i \sim \mathcal{N}(0, \triangle)$ for all $i = 1, 2, .., 9$,

$\tilde{V}_n$ is a numerical solution of $V_m(t_n)$,

$\tilde{x}1_n$ is a numerical solution of $x_1(t_n)$,

$\tilde{x}2_n$ is a numerical solution of $x_2(t_n)$,

$\tilde{x}3_n$ is a numerical solution of $x_3(t_n)$,

$\tilde{x}4_n$ is a numerical solution of $x_4(t_n)$,

$\tilde{x}5_n$ is a numerical solution of $x_5(t_n)$,

$\tilde{x}6_n$ is a numerical solution of $x_6(t_n)$,

$\tilde{x}7_n$ is a numerical solution of $x_7(t_n)$,

$\tilde{x}8_n$ is a numerical solution of $x_8(t_n)$,

$\tilde{x}9_n$ is a numerical solution of $x_9(t_n)$,

$\tilde{x}10_n$ is a numerical solution of $x_{10}(t_n)$,

for all $n = 1, 2, \ldots, N$.

3.3 The three aspects

In this work we simulate both models to analyze three aspects. They are the effect of I_{app} to the spike timing, the variability in spike timing, and interspike intervals. All of these aspects correlate with parameter σ which are very important because we add the term $x_i(t)(1 - x_i(t))$ at the random term for each SDE.

In this work, we study cerebellar granule cell which has threshold 11.5 cA. This threshold is used to divide the level of regularity or irregularity of firing. The initial conditions to simulate the process $V_m(t)$ for the original model are $\triangle = 10^{-3}$ s, $x_1(0) = x_2(0) = x_3(0) = x_4(0) = x_5(0) = x_6(0) = x_7(0) = x_8(0) = x_9(0) = 0.5, x_{10}(0) = 100 \times 10^{-6}$ and $V_m(0) = -0.07$ V. We use $\triangle = 10^{-3}$ because if we use $\triangle = 10^{-5}$ like in [2], we will not get any reasonable results.

3.3.1 The effect of I_{app} to the spike timing

For this aspect, we will simulate to see the effect of I_{app} to the spike timing. For the original model, we will use three values of I_{app} : $11, 12, 29\,cA$ with parameter $\sigma_i = \sigma = 0.5$ for $i = 1, 2, \ldots, 9$. For our model, we will use three values of I_{app} : $11, 12, 29\,cA$ with parameter $\sigma_i = \sigma = 0.5 \times 1000$ for $i = 1, 2, \ldots, 9$. For both models, we will simulate for $T = 0.4$ seconds.

3.3.2 The variability in spike timing

For this aspect, we will simulate to see the variability in spike timing which effected by the parameter σ. For the original model, we will use three values of $\sigma = 0.1, 0.3, 0.5$ with $I_{app} = 12\,cA$. For our model, we will use three values of $\sigma = 0.1 \times 1000, 0.3 \times 1000, 0.5 \times 1000$ with $I_{app} = 12\,cA$. We will simulate for 10 sample paths to see the variability. For each sample path, we will simulate for $T = 0.4$ seconds. The reason that we multiply the old parameter σ by 1000 is that in our model, we add the term $x_i(t)(1 - x_i(t))$'s to the stochastic part ; hence, the noises will be much smaller than usual. By our experiments, 1000 seems to be a good number to use for intensifying the degree of randomness for our model.

3.3.3 Interspike intervals

For this aspect, we will simulate to see the distribution of interspike intervals by using the distance between spikes that surpass the threshold $11.5\,cA$. For the original model, we will use three values of I_{app} : $11, 12, 29\,cA$ and three values of $\sigma = 0.1, 0.3, 0.5$. For our model, we will use three values of I_{app} : $11, 12, 29\,cA$ and three values of $\sigma = 0.1 \times 1000, 0.3 \times 1000, 0.5 \times 1000$ with $I_{app} = 12\,cA$ so that we have 9 cases in total. For each sample path, we will simulate for $T = 15$ seconds. Then, we plot histogram of interspike intervals for each case. After that, we use the coefficeint of variation (CV) to analyze the result. The CV of interspike intervals is used to quantify the regularity/irregularity of action potential firing. The CV is a standard measure of dispersion and is defined as the ratio of the standard deviation

to mean, i.e.

$$CV = \frac{Standard\,deviation}{Mean}.$$

Chapter 4

Results

This chapter presents the results from simulations in section 3. They are the effect of I_{app} to the spike timing, the variability in spike timing, and interspike intervals.

4.1 The effect of I_{app} to the spike timing

We use three values of I_{app} : 11, 12 and $29\,cA$ with the parameter $\sigma = 0.5$ for the original model and $\sigma = 0.5 \times 1000$ for our model. In each trace, firing is simulated for 0.4 seconds with a time step of 10^{-3} seconds.

Figure 4.1 and 4.2 show the behavior of stochastic granule cell model in response to three different deporarizing current pulses. In the upper panel, the depolarizing current is below the firing threshold ($I_{app} = 11\,cA$). In the middle panel, the depolarizing current is just above the firing threshold ($I_{app} = 12\,cA$). In the lower panel, the depolarizing current is considerably larger than the firing threshold ($I_{app} = 29\,cA$).

4.2 The variability in spike timing

We use three values of the parameter $\sigma = 0.1, 0.3$ and 0.5 for the original model, and $\sigma = 0.1 \times 1000, 0.3 \times 1000$ and 0.5×1000 for our model with $I_{app} = 12\,cA$. We will simulate for 10 sample paths to see the variability in spike timing. In each trace, firing is simulated for 0.4 seconds with a time step of 10^{-3} seconds.

Figure 4.3 and 4.4 show the variability in spike timing for the original model and

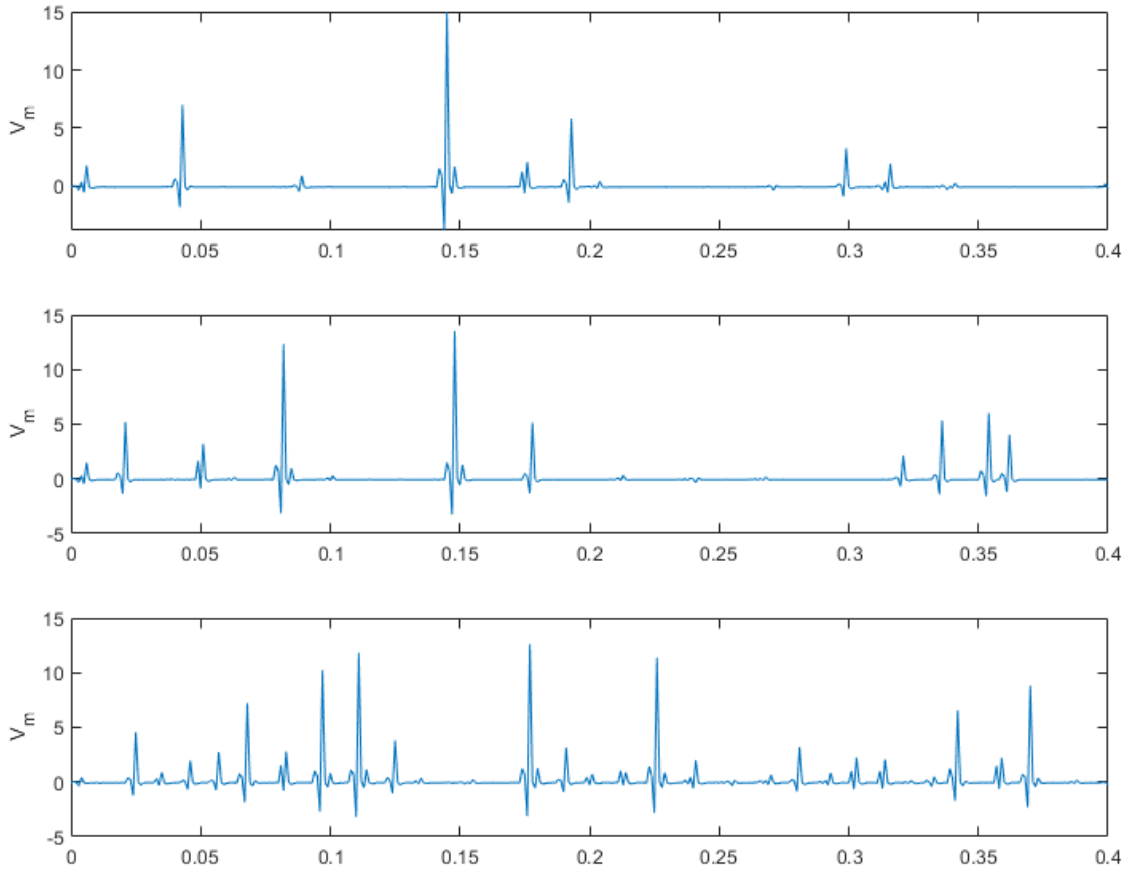

Figure 4.1: The effect of I_{app} to the spike timing for the original model.

our model, respectively. The upper panels correspond to $\sigma = 0.1$, the middle panels correspond to $\sigma = 0.3$, and the lower panels correspond to $\sigma = 0.5$. From figure 4.3, the value of the parameter σ affects spike timing. The higher the parameter σ is, the more variability spike timing will be. From figure 4.4, the value of the parameter σ affects spike timing. The higher the parameter σ is, the more variability in spike timing will be.

4.3 Interspike intervals

We will use three values of I_{app} = 11, 12 and $29\,cA$. We use three values of $\sigma = 0.1, 0.3$ and 0.5 for the original model and $\sigma = 0.1 \times 1000, 0.3 \times 1000$ and 0.5×1000 for our model. For each sample path, we will simulate for 15 seconds. We consider the time length between the peaks that surpass the threshold.

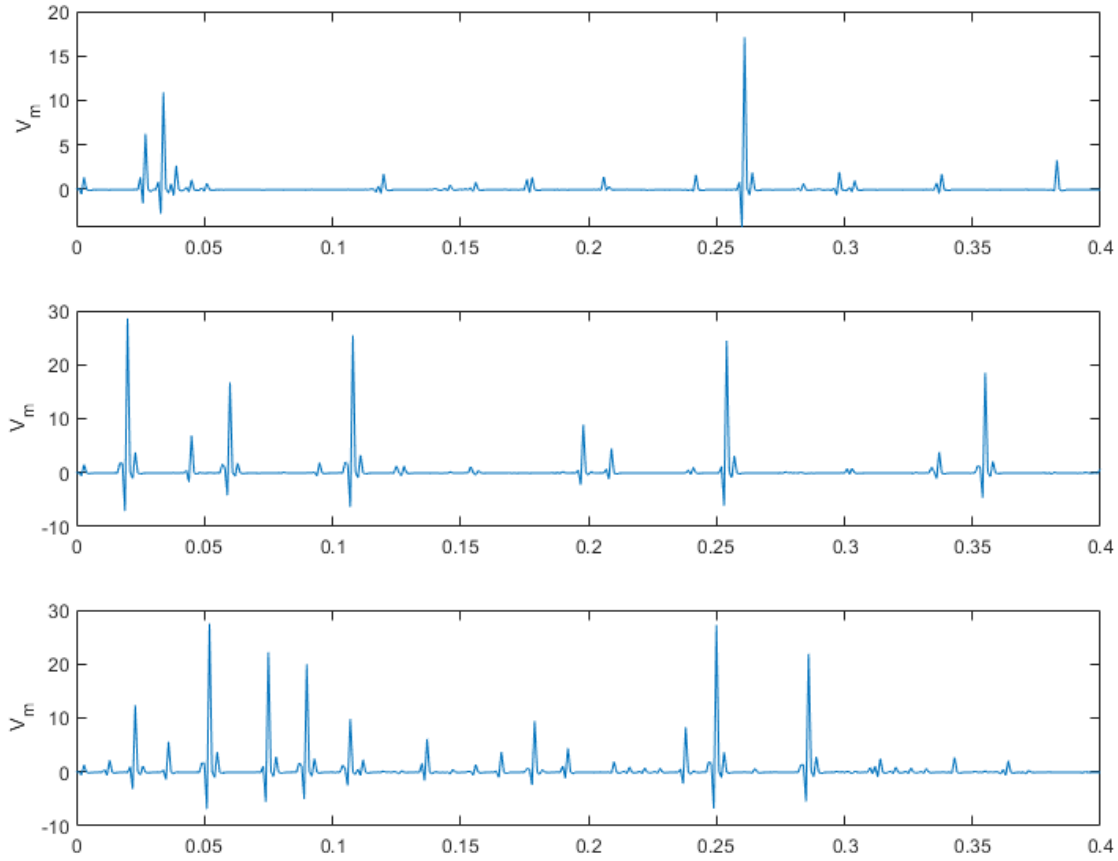

Figure 4.2: The effect of I_{app} to the spike timing for our model.

Figure 4.5 shows 9 histograms of interspike intervals. The top, middle, bottom panels correspond to the cases for I_{app} = 11, 12 and $29\,cA$, respectively. The left, middle, right panels correspond to the cases for $\sigma = 0.1, 0.3$ and 0.5, respectively.

For each case, the mean, standard deviation and the coefficient of variation of the interspike intevals are calculated and presented in figure 4.6. Seconds are used as the unit for the mean and the standard deviation, and the coefficient of variation is dimensionless.

Thr result from the original model is that if $I_{app} = 11\,cA$, the increase in the value of parameter σ increases the irregularity of firing measured by the value of CV. If $I_{app} = 12\,cA$, the increase in the value of the parameter σ increases the irregularity of firing measured by the value of CV. If $I_{app} = 29\,cA$, the increase in the value of parameter σ increases the regularity of firing measured by the value of CV.

Figure 4.7 shows 9 histograms of interspike intervals. The top, middle, bottom

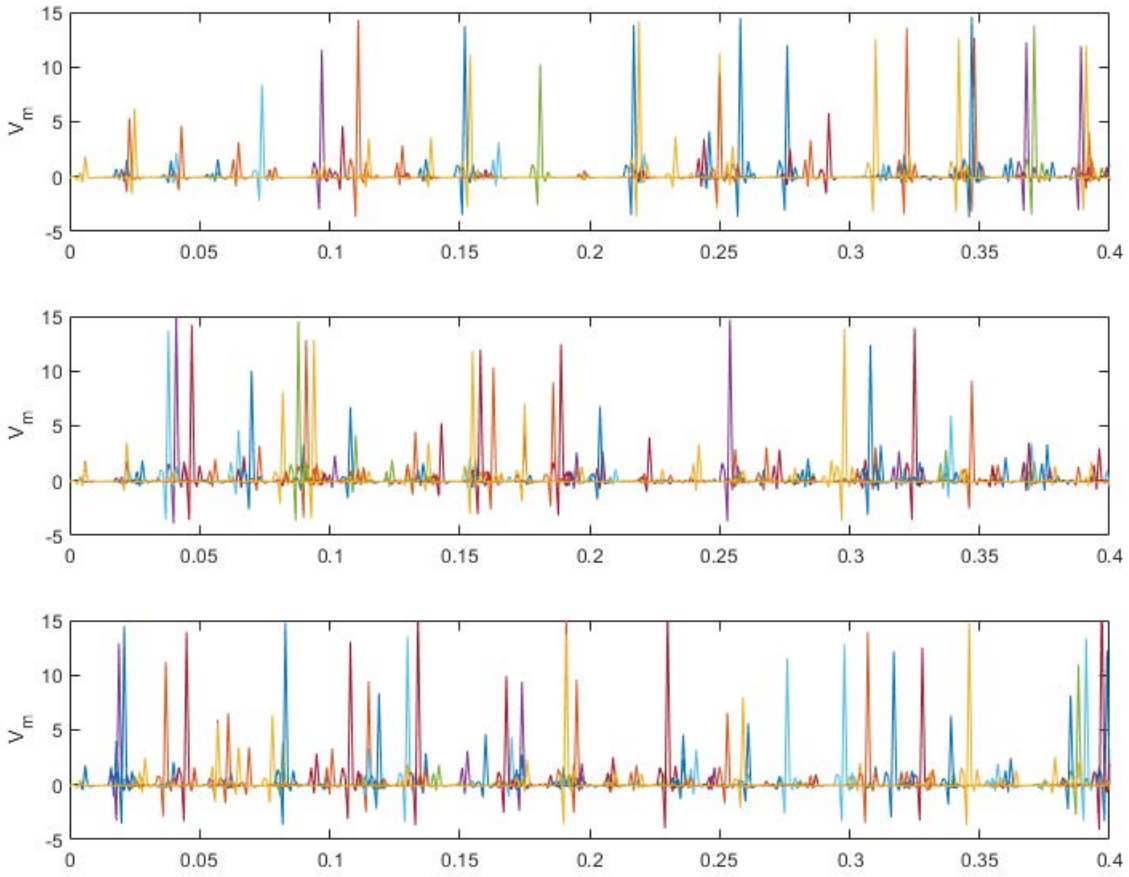

Figure 4.3: The variability in spike timing for the original model.

panels correspond to the cases for I_{app} = 11, 12 and 29 cA, respectively. The left, middle, right panels correspond to the cases for $\sigma = 0.1, 0.3$ and 0.5, respectively.

For each case, the mean, standard deviation and the coefficient of variation of the interspike intevals are calculated and presented in figure 4.8. Seconds are used as the unit for the mean and the standard deviation, and the coefficient of variation is dimensionless.

The result from our model is that if $I_{app} = 11\,cA$, the increase in the value of parameter σ increases the irregularity of firing measured by the value of CV. If $I_{app} = 12\,cA$, the increase in the value of parameter σ increases the irregularity of firing measured by the value of CV. If $I_{app} = 29\,cA$, the increase in the value of parameter σ increases the regularity of firing measured by the value of CV.

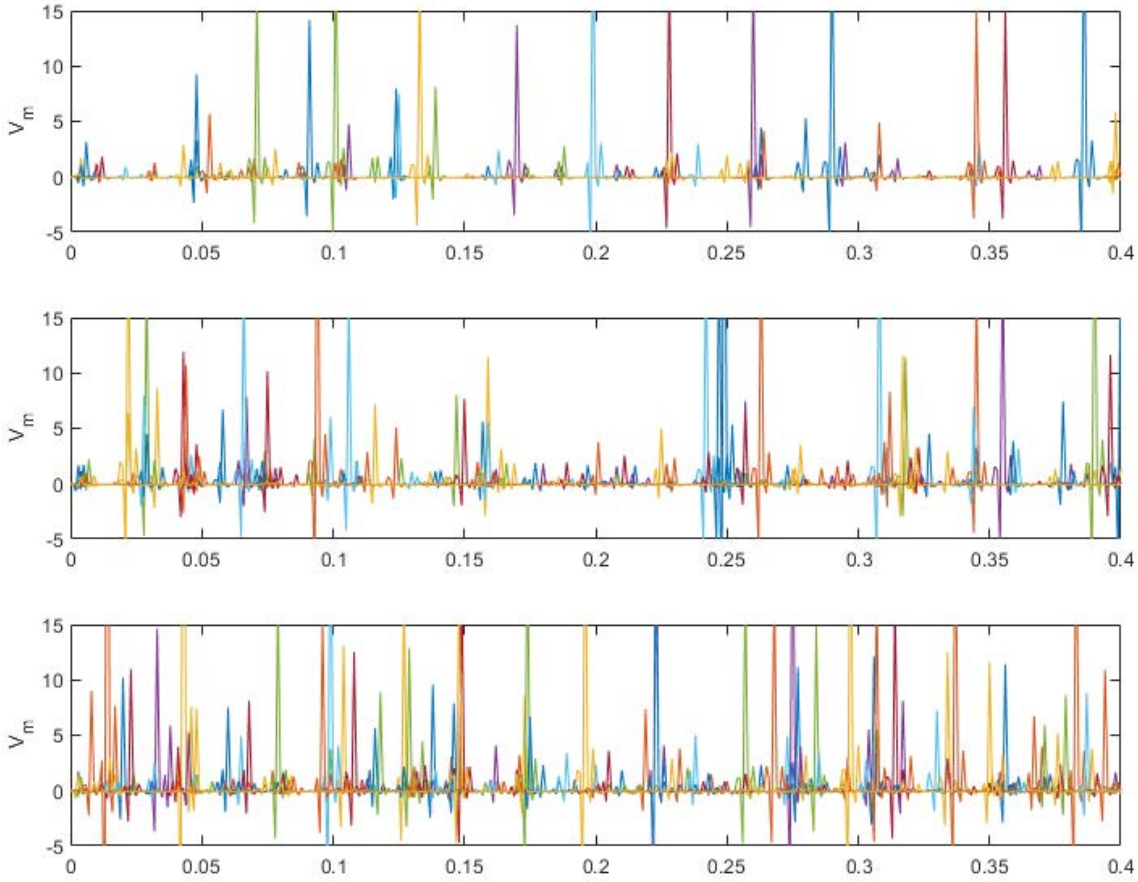

Figure 4.4: The variability in spike timing for our model.

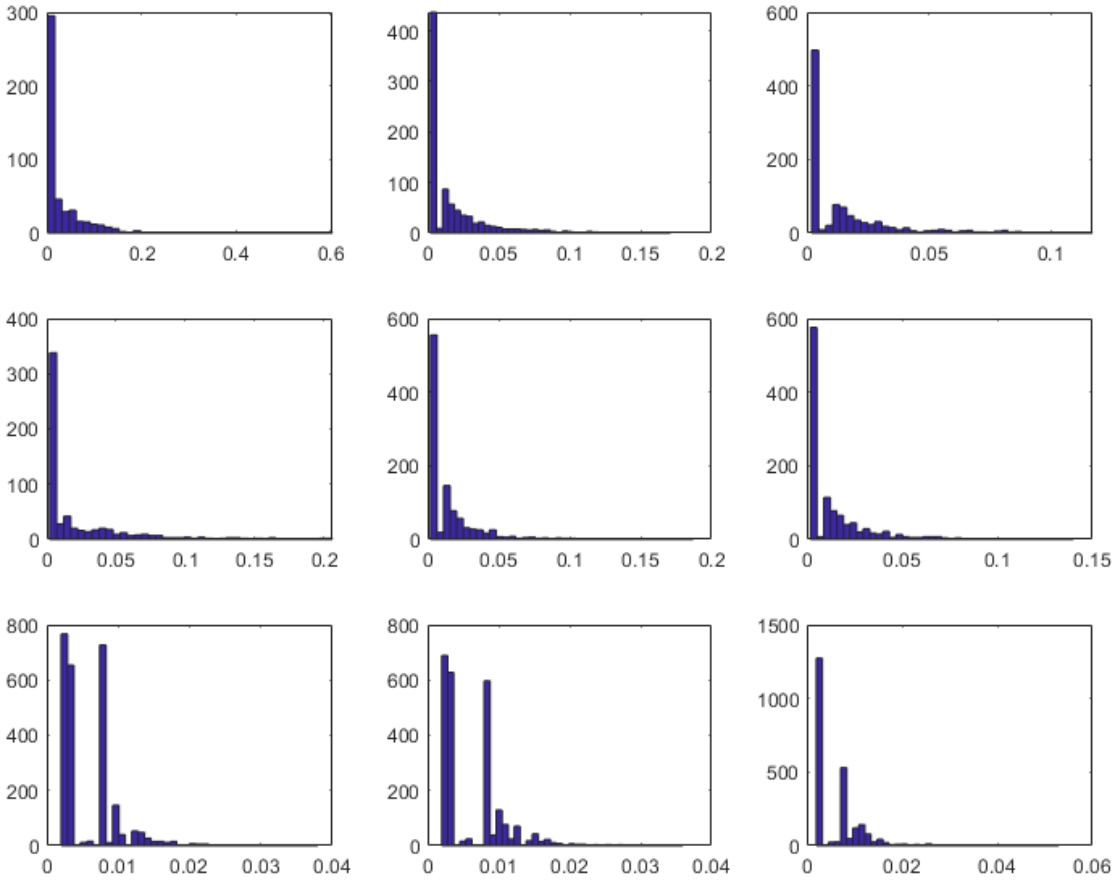

Figure 4.5: Histogram of interspike intervals for the original model.

Depolarizing current	sigma	mean(s)	std(s)	CV
I_{app}= 11 cA	0.1	0.0311	0.0514	0.6045
	0.3	0.0175	0.0229	0.7633
	0.5	0.0153	0.0193	0.7902
I_{app}= 12 cA	0.1	0.0243	0.037	0.6559
	0.3	0.0144	0.0192	0.7525
	0.5	0.0136	0.0171	0.7981
I_{app}= 29 cA	0.1	0.0058	0.0044	1.3086
	0.3	0.0061	0.0048	1.2718
	0.5	0.0062	0.005	1.2511

Figure 4.6: Quantitative analysis of the interspike intervals of original model.

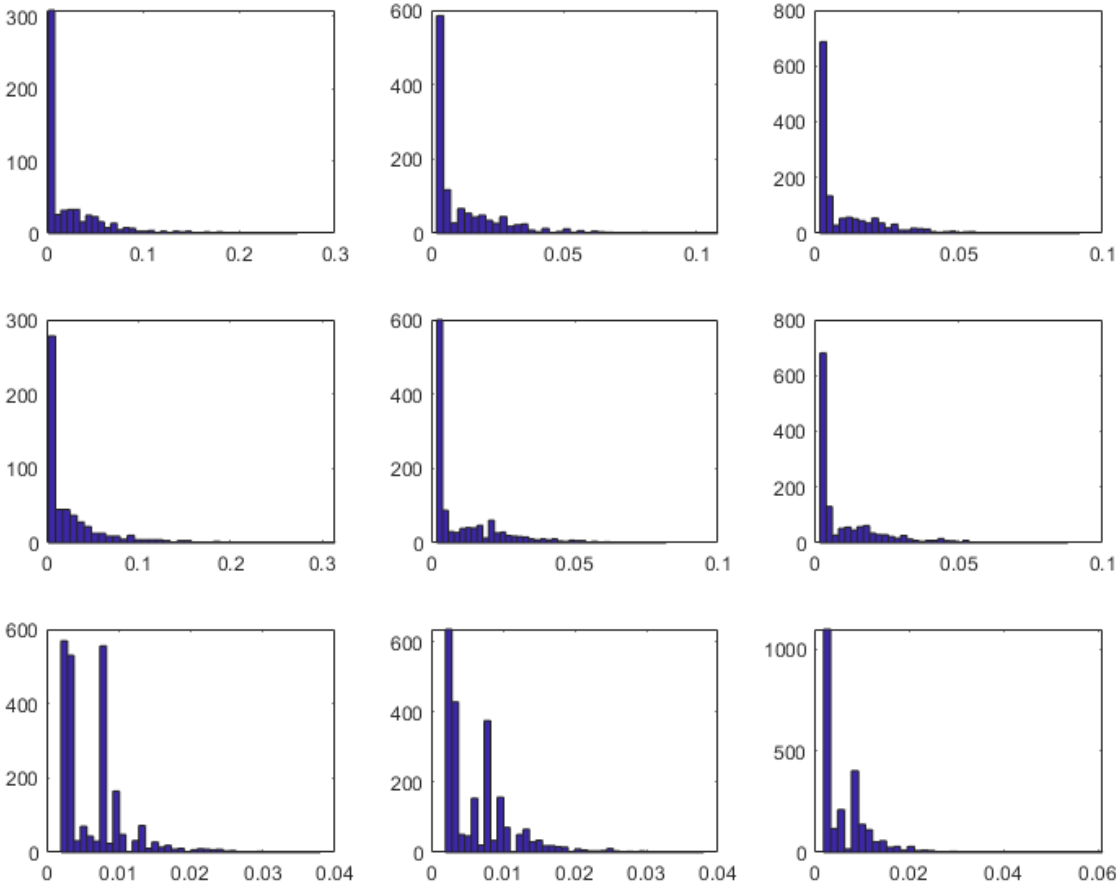

Figure 4.7: Histogram of interspike intervals for our model.

Depolarizing current	sigma	mean(s)	std(s)	CV
I_{app}= 11 cA	0.1	0.0311	0.0514	0.6045
	0.3	0.0175	0.0229	0.7633
	0.5	0.0153	0.0193	0.7902
I_{app}= 12 cA	0.1	0.0243	0.037	0.6559
	0.3	0.0144	0.0192	0.7525
	0.5	0.0136	0.0171	0.7981
I_{app}= 29 cA	0.1	0.0058	0.0044	1.3086
	0.3	0.0061	0.0048	1.2718
	0.5	0.0062	0.005	1.2511

Figure 4.8: Quantitative analysis of the interspike intervals of our model.

Chapter 5

Conclusion

As for the original model, if we increase the value of I_{app}, the firing will occur more frequently. The value of parameter σ affects spike timing. The higher the parameter σ is, the more variability spike timing will be. We use coefficeint of variation (CV) to analyze the result. The CV of interspike intervals is often to quantify the regularity or irregularity of action potential firing. The increase in the value of parameter σ increases the regularity of firing measured by the value of CV. However, our result does not coincide with the result in [2]. In [2], the result is that if $I_{app} = 11\,cA$, the increase in the value of parameter σ increases the regularity of firing measured by the value of CV. If $I_{app} = 12, 29\,cA$, the increase in the value of parameter σ increases the irregularity of firing measured by the value of CV but our result is that if $I_{app} = 11\,cA$, the increase in the value of parameter σ increases the regularity of firing measured by the value of CV. If $I_{app} = 12, 29\,cA$, the increase in the value of parameter σ increases the irregularity of firing measured by the value of CV but our result is that if $I_{app} = 11\,cA$, the increase in the value of parameter σ increases the irregularity of firing measured by the value of CV. If $I_{app} = 12\,cA$, the increase in the value of parameter σ increases the irregularity of firing measured by the value of CV. If $I_{app} = 29\,cA$, the increase in the value of parameter σ increases the regularity of firing measured by the value of CV. There are four possible reasons for this problem.

The first reason is that there are no initial conditions provided in [2]. In this work, we choose the initial condition for all processes $x_i(t)$'s to be 0.5 for $i = 1, 2, \ldots, 9$. The initial condition for $x_{10}(t)$ is chosen to be 100×10^{-6}.The initial condition for the

process $V_m(t)$ is chosen to be -0.07 which can be found in [1]. The second reason is that in [2], there is one additional ion process, which is the inactive BK_{Ca} ion process, appearing in the equation for the process V_m. However, there is no equation for the inactive BK_{Ca} ion process in the model. Thus, in this work, we exclude the inactive BK_{Ca} ion process from the model. The third reason is that, from (1), the unit for the terms $\frac{BG_5 x_7^{p5}(t) x_8^{q5}(t)(V_m(t)-E_5)}{\pi dcell^2 dshell}$ and $\frac{x_{10}(t)-[Ca^{2+}]_{rest}}{\tau_{Ca}}$ are different. There may be some additional parameters to add in the equation for the x_{10} process. The fourth reason is that we use a time step of 10^{-3} instead of 10^{-5} from the original model. Here, from the first and second reasons above, if the inactive BK_{Ca} ion process does not appear in the model and there is no additional parameter to add in the equation for x_{10} process, we cannot get any reasonable result by using the time step of 10^{-5}.

As for our model, if we increase the value of I_{app}, the firing will occur more frequently. However, the value of $I_{app} = 11\,cA$ does not coincide with the result in [2]. The value of parameter σ affects spike timing. The higher the parameter σ is, the more variability spike timing will be. The increase in the value of the parameter σ increases the regularity of firing measured by the value of CV. Our result is that if $I_{app} = 11\,cA$, the increase in the value of the parameter σ increases the irregularity of firing measured by the value of CV. If $I_{app} = 12\,cA$, the increase in the value of parameter σ increases the irregularity of firing measured by the value of CV. If $I_{app} = 29\,cA$, the increase in the value of the parameter σ increases the regularity of firing measured by the value of CV.

The reason for every problem arisen in our model is that the parameters that are used may be not suitable for our model. Thus, we may need to do another scientific experiment in order to find suitable parameters for our model.

References

[1] Linne M-L, Jalonen TO, Simulation of the cultured granule neuron excitability, *Neurocomputing* **52-54**(2003): 583–590.

[2] Saarinen A, Linne M-L, Yli-Harja O , Stochastic differential equation model for cerebellar granule cell excitability, *PLoS Comput Biol* **4**(2008): 1–11.

[3] Saarinen A, Linne M-L, Yli-Harja O, Modeling single neuron behavior using stochastic differential equations, *Neurocomputing* **69**(2006): 1091–1096.

The Project Proposal of Course 2301399 Project Proposal
Academic Year 2018

Project Title (Thai)	ก้ารจำลองตัวแบบสมการเชิงอนุพันธ์สโตแคสติกสำหรับการตอบสนองต่อสิ่งกระตุ้นของเซลล์แกรนูลในสมองส่วนซีรีเบลลัม
Project Title (English)	Simulations of Stochastic Differential Equation Model for Cerebellar Granule Cell Excitability
Project Advisor	Professor Raywat Tanadkithirun, Ph.D.
By	Sornthuss Kawinnitipan ID 5833523523 Mathematics, Department of Mathematics and Computer Science, Chulalongkorn University

---

Background and Rationale and Scope

Neurons are electrically excitable cells that receive, process, and transmit information through electrical and chemical signals. Neurons in the brain express intrinsic dynamic behavior which is known to be stochastic in nature. Cerebellar granule cells are the most abundant neurons in the human brain and are among the smallest neurons in the brain.

In the cell membrane, many ions have a concentration gradient across the membrane. Some ions have high concentration inside the membrane but low concentration outside the membrane, and vice versa. These concentration gradients provide the potential energy to drive the formation of the membrane potential. This voltage is established when the membrane has permeability to one or more ions.

Ion channels are pore-forming membrane proteins that allow ions to pass through the channel pore. Due to random opening and closing (gating) of an ion channel at an experimentally fixed membrane potential, Saarinen et al. [2] propose a system of stochastic differential equations (SDEs) to model the intrinsic dynamic behavior of cerebellar granule cells. This model includes six different types of voltage-dependent conductances: the fast inactivating sodium channel (Na_F), the delayed rectifier potassium channel (K_{D_r}), the transient A-type potassium channel (K_A), the inward rectifier potassium channel (K_{i_r}), the high-voltage-activated calcium chan-

nel (Ca_{HVA}), and the large-conductance calcium and voltage-activated potassium channel (BK_{ca}).The change in membrane potential is described by

$$\left.\begin{aligned}
dV_m(t) &= \frac{1}{C_m}\Big(I_{app} - G_1 x_1^{p_1}(t)x_2^{q_1}(t)(V_m(t)-E_1) \\
&\qquad - G_2 x_3^{p_2}(t)(V_m(t)-E_2) - G_3 x_4^{p_3}(t)x_5^{q_3}(t)(V_m(t)-E_3) \\
&\qquad - G_4 x_6^{p_4}(t)(V_m(t)-E_4) - G_5 x_7^{p_5}(t)x_8^{q_5}(t)(V_m(t)-E_5) \\
&\qquad - G_6 x_9^{p_6}(t)(V_m(t)-E_6) - \frac{1}{R_m}(V_m(t)-E_m)\Big)dt, \\
dx_1(t) &= \big(\alpha_1(V_m(t))(1-x_1(t)) - \beta_1(V_m(t))x_1(t)\big)dt + \sigma_1 dW_1(t), \\
dx_2(t) &= \big(\alpha_2(V_m(t))(1-x_2(t)) - \beta_2(V_m(t))x_2(t)\big)dt + \sigma_2 dW_2(t), \\
dx_3(t) &= \big(\alpha_3(V_m(t))(1-x_3(t)) - \beta_3(V_m(t))x_3(t)\big)dt + \sigma_3 dW_3(t), \\
dx_4(t) &= \big(\alpha_4(V_m(t))(1-x_4(t)) - \beta_4(V_m(t))x_4(t)\big)dt + \sigma_4 dW_4(t), \\
dx_5(t) &= \big(\alpha_5(V_m(t))(1-x_5(t)) - \beta_5(V_m(t))x_5(t)\big)dt + \sigma_5 dW_5(t), \\
dx_6(t) &= \big(\alpha_6(V_m(t))(1-x_6(t)) - \beta_6(V_m(t))x_6(t)\big)dt + \sigma_6 dW_6(t), \\
dx_7(t) &= \big(\alpha_7(V_m(t))(1-x_7(t)) - \beta_7(V_m(t))x_7(t)\big)dt + \sigma_7 dW_7(t), \\
dx_8(t) &= \big(\alpha_8(V_m(t))(1-x_8(t)) - \beta_8(V_m(t))x_8(t)\big)dt + \sigma_8 dW_8(t), \\
dx_9(t) &= \big(\alpha_9(V_m(t),x_{10}(t))(1-x_9(t)) - \beta_9(V_m(t),x_{10}(t))x_9(t)\big)dt + \sigma_9 dW_9(t), \\
dx_{10}(t) &= \Big(\frac{B\,G_5 x_7^{p_5}(t)x_8^{q_5}(t)(V_m(t)-E_5)}{\pi\, dcell^2\, dshell} - \frac{x_{10}(t)-[Ca^{2+}]_{rest}}{\tau_{Ca}}\Big)dt,
\end{aligned}\right\} \quad (1)$$

From a suggestion in [2], we also add stochasticity into gating variables to obtain another model. In this work, we will simulate the process $V_m(t)$ by using the Euler-Maruyama method and use the result to analyze the variability in spike timing and interspike intervals.

Objectives

1. To generalize the original model (1).
2. To study how to use a numerical method to simulate the process of membrane potential using the original model and the generalized model.
3. To analyze the variability in spike timing and interspike intervals.

Project Activities

1. Study the articles [1] and [2].
2. Search for related information.
3. Study the SDE model from [1]
4. Simulate the models by using the Euler-Maruyama method.
5. Use the result to analyze the variability in spike timing and interspike intervals.
6. Investigate the result from the simulation.
7. Make a conclusion and write the report.

Activities Table

Project Activities	August 2561 - April 2562								
	Aug	Sep	Oct	Nov	Dec	Jan	Feb	Mar	Apr
1. Study the articles [1] and [2].									
2. Search for related information.									
3. Study SDE model from [1]									
4 . Simulate the models by using the EM method.									
5. Use the result to analyze the variability in spike timing and interspike intervals.									
6. Investigate the result from the simulation.									
7. Make a conclusion and write the report.									

Benefits

1. Be able to simulate the sophisticated system of SDEs.
2. Know how to implement the Euler-Maruyama method

Equipment

1. A4 paper
2. A Laptop
3. Microsoft Word, MathType, MATLAB and Mathematica
4. Journals and related books

References

[1] Linne M-L, Jalonen TO, Simulation of the cultured granule neuron excitability, *Neurocomputing* **52-54**(2003): 583–590.

[2] Saarinen A, Linne M-L, Yli-Harja O , Stochastic differential equation model for cerebellar granule cell excitability, *PLoS Comput Biol* **4**(2008): 1–11.

[3] Saarinen A, Linne M-L, Yli-Harja O, Modeling single neuron behavior using stochastic differential equations, *Neurocomputing* **69**(2006): 1091–1096.

Biography

Mr. Sornthuss Kawinnitipan ID:5833523523

Branch of Mathematics

Department of Mathematics and Computer Science

Chulalongkorn University